

1-1-2011

Compositional study of vacuum annealed Al doped ZnO thin films obtained by RF magnetron sputtering

B. P. Shantheyanda
University of Central Florida

V. O. Todi
University of Central Florida

K. B. Sundaram
University of Central Florida

A. Vijayakumar

I. Oladeji

Find similar works at: <https://stars.library.ucf.edu/facultybib2010>
University of Central Florida Libraries <http://library.ucf.edu>

This Article is brought to you for free and open access by the Faculty Bibliography at STARS. It has been accepted for inclusion in Faculty Bibliography 2010s by an authorized administrator of STARS. For more information, please contact STARS@ucf.edu.

Recommended Citation

Shantheyanda, B. P.; Todi, V. O.; Sundaram, K. B.; Vijayakumar, A.; and Oladeji, I., "Compositional study of vacuum annealed Al doped ZnO thin films obtained by RF magnetron sputtering" (2011). *Faculty Bibliography 2010s*. 1894.
<https://stars.library.ucf.edu/facultybib2010/1894>

Compositional study of vacuum annealed Al doped ZnO thin films obtained by RF magnetron sputtering

B. P. Shantheyanda, V. O. Todi, K. B. Sundaram, A. Vijayakumar, and I. Oladeji

Citation: *Journal of Vacuum Science & Technology A* **29**, 051514 (2011); doi: 10.1116/1.3624787

View online: <https://doi.org/10.1116/1.3624787>

View Table of Contents: <https://avs.scitation.org/toc/jva/29/5>

Published by the [American Vacuum Society](#)

ARTICLES YOU MAY BE INTERESTED IN

[A comprehensive review of ZnO materials and devices](#)

Journal of Applied Physics **98**, 041301 (2005); <https://doi.org/10.1063/1.1992666>

[Effect of sputtering power on crystallinity, intrinsic defects, and optical and electrical properties of Al-doped ZnO transparent conducting thin films for optoelectronic devices](#)

Journal of Applied Physics **121**, 085302 (2017); <https://doi.org/10.1063/1.4977104>

[Influence of RF power on magnetron sputtered AZO films](#)

AIP Conference Proceedings **1512**, 764 (2013); <https://doi.org/10.1063/1.4791262>

[Transparent ZnO thin-film transistor fabricated by rf magnetron sputtering](#)

Applied Physics Letters **82**, 1117 (2003); <https://doi.org/10.1063/1.1553997>

[Preparation and properties of transparent conductive aluminum-doped zinc oxide thin films by sol-gel process](#)

Journal of Vacuum Science & Technology A **19**, 1642 (2001); <https://doi.org/10.1116/1.1340659>

[Structural, electrical and optical properties of aluminum doped zinc oxide films prepared by radio frequency magnetron sputtering](#)

Journal of Applied Physics **81**, 7764 (1997); <https://doi.org/10.1063/1.365556>



Instruments for Advanced Science


Contact Hiden Analytical for further details:
W www.HidenAnalytical.com
E info@hiden.co.uk

CLICK TO VIEW our product catalogue



Gas Analysis

- dynamic measurement of reaction gas streams
- catalysis and thermal analysis
- molecular beam studies
- dissolved species probes
- fermentation, environmental and ecological studies



Surface Science

- UHV TPD
- SIMS
- end point detection in ion beam etch
- elemental imaging - surface mapping



Plasma Diagnostics

- plasma source characterization
- etch and deposition process reaction kinetic studies
- analysis of neutral and radical species



Vacuum Analysis

- partial pressure measurement and control of process gases
- reactive sputter process control
- vacuum diagnostics
- vacuum coating process monitoring

Compositional study of vacuum annealed Al doped ZnO thin films obtained by RF magnetron sputtering

B. P. Shantheyanda, V. O. Todi, and K. B. Sundaram

Department of Electrical Engineering and Computer Science, University of Central Florida,
Orlando, Florida 32816

A. Vijayakumar^{a)} and I. Oladeji

Planar Energy Inc., 653 W. Michigan St., Orlando, Florida 32805

(Received 28 March 2011; accepted 8 July 2011; published 18 August 2011)

Aluminum doped zinc oxide (AZO) thin films were obtained by RF magnetron sputtering. The effects of deposition parameters such as power, gas flow conditions, and substrate heating have been studied. Deposited and annealed films were characterized for composition as well as microstructure using x ray photoelectron spectroscopy and x ray diffraction. Films produced were polycrystalline in nature. Surface imaging and roughness studies were carried out using SEM and AFM, respectively. Columnar grain growth was predominantly observed. Optical and electrical properties were evaluated for transparent conducting oxide applications. Processing conditions were optimized to obtain highly transparent AZO films with a low resistivity value of $6.67 \times 10^{-4} \Omega \text{ cm}$. © 2011 American Vacuum Society. [DOI: 10.1116/1.3624787]

I. INTRODUCTION

Transparent conductive oxide (TCO) thin films have a wide range of applications, such as transparent front electrodes in photovoltaic cells, flat panel displays, low-emissivity windows, electrochromic mirrors and windows, defrosting windows, and electromagnetic shielding.¹⁻³ In the TCO family, indium tin oxide (ITO) has been the most popular choice due its superior electrical and optical properties for most practical applications. However, due to the limited availability of Indium in nature, the production cost for ITO based TCOs has increased drastically.⁴ Binary compounds such as CdO, ZnO, and SnO₂ can also be used as transparent conducting films. Nevertheless, the instability of most of these binary compounds at higher temperatures keeps them from being used as transparent electrodes for practical applications.⁵

It is essential to come up with low cost replacements to ITO in most applications due to the relative boom in demand. Impurity doping of the alternative binary compounds have been known to yield films with good thermal stability and lower resistivity. Zinc oxide (ZnO) is considered as a promising candidate for impurity doping, while, improvements in properties of the films obtained using other binary compounds were less significant. The properties of zinc oxide such as good stability in hydrogen plasma ambient, good thermal stability when doped with group-III elements, nontoxicity, wide band gap ($\sim 3.3 \text{ eV}$), and high conductivity make it an attractive candidate for many applications. In particular, aluminum doped ZnO thin films have shown great potential for TCO applications with significant drop in resistivity values. Furthermore, easy dopability as well as abundant availability of zinc has enabled its choice as a lower cost alternative for TCO applications.^{6,7}

TCO thin films with better electrical properties always depend on the preparation conditions and techniques. Some of the methods used to deposit AZO thin films are chemical beam deposition,⁸ chemical vapor deposition,^{9,10} pulsed laser deposition,^{11,12} dc magnetron sputtering,¹³ spray pyrolysis technique,¹⁴ ion beam assisted reactive deposition,¹⁵ e-beam evaporation,¹⁶ and sol-gel process.^{17,18} Among these techniques, dc and RF sputtering are the most promising due to the high degree of control that can be exercised over the deposition parameters. Preparation of low resistivity AZO thin films using dc magnetron sputtering depends on the oxygen content in the ZnO:Al target and the amount of oxygen generated from the target reaching the substrate surface.¹³ Zinc is more chemically active in oxidizing atmospheres than tin and indium, which makes it more difficult to control during the oxide formation process when compared to other binary compounds such as SnO₂ and In₂O₃.¹⁹ Furthermore, the target erosion pattern created during sputtering affects the activity and quantity of oxygen that can reach the substrate surface. This causes randomness in the resistivity values observed at different parts of the deposited film.¹⁴ Research has been carried out to partially overcome this issue of dc magnetron sputtering by placing the target perpendicular to the substrate and applying a magnetic field during deposition.^{20,21} Kluth *et al.* have reported the use of RF magnetron sputtering to produce uniform AZO films. In their studies, the properties of RF sputtered AZO films showed a weak dependence on film thickness and substrate temperature while a strong dependence on sputter pressure and oxygen addition to the process gas is observed.²²

Previous work has been reported on the preparation of RF sputtered ZnO:Al thin films using different gas flow conditions, sputter pressures, substrate heating, and varying percentages of Al₂O₃ in the sputtering target.^{23,24} The sputter deposited Al doped ZnO thin films are annealed under vacuum in order to achieve lower electrical resistivity values.^{25,26} Aluminum doping is expected to increase free

^{a)}Author to whom correspondence should be addressed; electronic mail: arunv@planarenergy.com

carrier concentration and thus improve the resistivity of the films. Chen *et al.* have reported the effects of compositional changes on the chemical state of oxygen and aluminum in vacuum annealed AZO films obtained by dc sputtering.²⁷ Similarly, the influence of post-deposition annealing on the electrical and optical properties of transparent conductive AZO thin films prepared by RF magnetron sputtering was reported by Fang *et al.*,²⁸ Berginski *et al.*,²⁶ have discussed on the effects of vacuum annealing on the electrical properties of RF sputtered AZO thin films with carrier mobility measurements. They have reported a decrease in resistivity of the films with vacuum annealing and found that film quality and annealing temperature play an important role in determining the resistivity.

Lu *et al.* prepared Al-doped ZnO thin films by mist chemical vapor deposition and magnetron sputtering. They studied the band gap shift as a function of carrier concentration and observed an increase in band gap with carrier concentration.²⁹ The same group also reported on (Zn:Al)O thin films prepared by a dc magnetron sputtering with Al contents in the range of 0–50 at. %. Their systematic study on the structural, optical and electrical properties of these films, revealed that optimum results were obtained at an Al content of 4 at. % with low resistivity $\sim 10^{-3}$ Ω cm, high transmittance $\sim 90\%$ in the visible region and crystal quality with a high c-axis orientation.³⁰ However, there is a lack of knowledge about the compositional changes of RF sputtered AZO thin films after annealing in vacuum. Understanding the exact nature of chemical changes occurring in the material due to the annealing process can help to tailor these films to achieve desired properties. In this paper, we present a detailed compositional study of the annealed AZO thin films prepared by radio frequency magnetron sputtering. Variation of sputtering parameters such as deposition power and substrate heating are also considered for the studies. XPS analysis is carried out to analyze film compositional changes. The most optimum deposition and post deposition annealing process conditions are identified to tune the optical, electrical, and structural properties for the films for TCO applications.

II. EXPERIMENT

ZnO:Al films were deposited on Si/SiO₂ and glass substrates for various studies. The films were deposited by RF magnetron sputtering in a multigun ultra-high vacuum sputtering system manufactured by AJA International. A 3 in. diameter target consisting of zinc oxide with 3 wt. % of Al₂O₃ was used. Initially the system was evacuated to a base pressure in the 1×10^{-7} Torr range. Argon gas flow in the chamber was kept constant at 10 sccm and the deposition pressure was maintained at 5 mTorr for all depositions. The substrate holder was placed 21 cm away from the target and was rotated axially at 20 rpm in order to improve the uniformity of the deposited films. The power applied was varied in the range of 125–175 W and substrate temperatures of 200 and 250 °C were used during the depositions. The duration of all depositions was fixed at 90 min and the film thickness was measured using an Alpha-Step 500 Surface Profilometer.

The deposited AZO thin films were subsequently annealed for 15 min in vacuum up to 400 °C at increments of 50 °C for different sets of samples. The base pressure of the chamber during vacuum annealing was kept at 4.1×10^{-7} Torr. Resistivity was measured using four-point probe technique.

A Cary-500 UV-visible spectrophotometer was used to study the optical transmission characteristics of the thin film samples. This is a double beam instrument controlled by a microprocessor and has a measurement range of 3000 to 300 nm. X-ray photoelectron spectroscopy (XPS) was performed using a PHI 5400 ESCA system. The base pressure during analysis was in the 10^{-9} Torr range and Mg K α x ray source ($h\nu = 1253.6$ eV) at a power of 300 W was used for the analysis. The surface analytical studies were typically performed on the films deposited on Si wafers. Both the survey and the high-resolution spectra were recorded with electron pass energies of 44.75 and 35.75 eV, respectively, to achieve the maximum spectral resolution. Any charging shift produced by the samples was carefully removed by calibration of the binding energy scale to the hydrocarbon part of the C (1s) adventitious carbon line at 284.6 eV. Nonlinear least square curve fitting was performed using a Gaussian/Lorentzian peak shape after the background removal. Scanning electron microscopy (SEM) images of the deposited thin film was taken using Hitachi S3500N. Atomic force microscopy (AFM) was used to measure the roughness of deposited films using Molecular Imaging Pico SPM AFM tool. Crystal structure of the films was studied using a Rigaku D-Max B, x ray diffraction (XRD) tool.

III. RESULTS AND DISCUSSION

Figure 1 shows the deposition rate of aluminum doped zinc oxide films as a function of deposition power and substrate temperature. It can be observed that the deposition rate continuously increases with applied power for substrate temperatures 200 and 250 °C, respectively. This increase in deposition rate indicates that the number of atoms sputtered

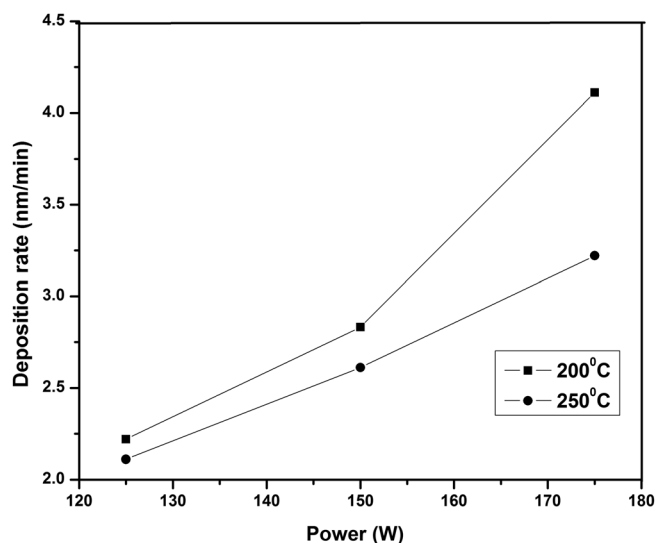


FIG. 1. Deposition rate with respect to power of deposition at different substrate temperatures.

from the target is proportional to the increase in the RF power. Furthermore, it can be seen that the deposition rates are lower for the films deposited at higher substrate temperatures. This is attributed to the increase in the number of atoms leaving the substrate surface due to thermal desorption. It has been reported that limited surface mobility of adatoms at low substrate temperatures also leads to higher growth rate.³¹

X-ray diffraction spectra obtained for the AZO thin films are shown in Figs. 2(a) and 2(b) at various deposition powers for 200 and 250 °C substrate temperatures respectively. The diffraction spectra indicate that these films have polycrystalline hexagonal wurtzite structure with an orientation perpendicular (002) to the substrate surface (*c*-axis orientation) at 34.4° (2 θ). The large peak observed at 34.4° determines the presence of (002) crystal orientation in the deposited films. Some of these films showed smaller peaks at 36.25° and 38.35° indicating (101) and (202) texture growth. The XRD peaks appear to be more intense at lower powers for films deposited at both substrate temperatures. This indicates better crystallinity in the films deposited at lower power con-

ditions. Furthermore, the FWHM of the peaks increases with increase in deposition power, indicating a decrease in grain size of the deposited films. Additionally no significant shifts were observed in the measured diffraction peaks. Any such change in diffraction peak position could be attributed to the amount of aluminum incorporation in the film.³² Hence, it can be inferred that the films have minimal incorporation of aluminum with grain size in the range of 15–20 nm.

Figure 3 shows the SEM cross section images of AZO films obtained under different deposition conditions. The images clearly show the columnar grain growth that starts from the substrate surface as reported previously by Sundaram *et al.*³³ and Dinescu *et al.*³⁴ The columnar growth is more prominent for the films obtained at lower powers. Additionally, the width of these columnar grains increases with increase in the deposition power, irrespective of substrate temperature variation. The width of these columnar structures are larger for the AZO films deposited at 250 °C substrate temperature compared to that of the film deposited at 200 °C. Also, the film microstructure agrees well with the trend explained by Thornton's structure zone model for sputtered metallic films.³⁵ The model identifies four zones in the surface structure as a function of argon pressure and substrate temperature. A modified version of the structure zone model was proposed by Kluth *et al.* due to the difference in the properties between TCO and metals.³⁶ The modification to the model was proposed taking into account the low probability of recrystallization occurring in ZnO films since substrate temperatures during deposition are much lower when compared to recrystallization temperatures. AFM studies indicated an average surface roughness in the range of 20 nm and seemed to decrease to less than 10 nm at higher deposition powers. This could be a direct consequence of the change in structure of the film with larger columnar grains promoting smoother grain surface.

XPS survey scans indicate that zinc and aluminum content in the films increases with the increase in deposition power as well as substrate temperature. Figure 4 shows the concentration of Al in the films with respect to the deposition powers. It is seen that the Al content increased slightly with the increase in deposition power and the films deposited at 250 °C have higher concentration of Al when compared to the films deposited at 200 °C. However, the oxygen concentration in the films was observed to decrease with increasing power and substrate temperature. These compositional changes play an important role in determining the electrical and optical properties of the films. Hence we considered the high resolution scans for each element to understand the bonding states. Figure 5 shows the oxygen (O1s) photoelectron peaks in the XPS spectra of AZO films prepared at 125 W and 200 °C substrate heating temperature. The O1s peak is composed of four sub peaks (OI, OII, OIII, and OIV). The peak OI at 530.4 ± 0.1 eV is attributed to the O^{2-} ions on the wurtzite structure of hexagonal Zn^{+} ion array. In other words these include O^{2-} ions surrounded by Zn atom with their full compliment.^{37–39} The O^{2-} ions in the oxygen deficient regions of the ZnO matrix is located at 531.4 ± 0.10 eV (OII).⁴⁰ The binding energy component located at

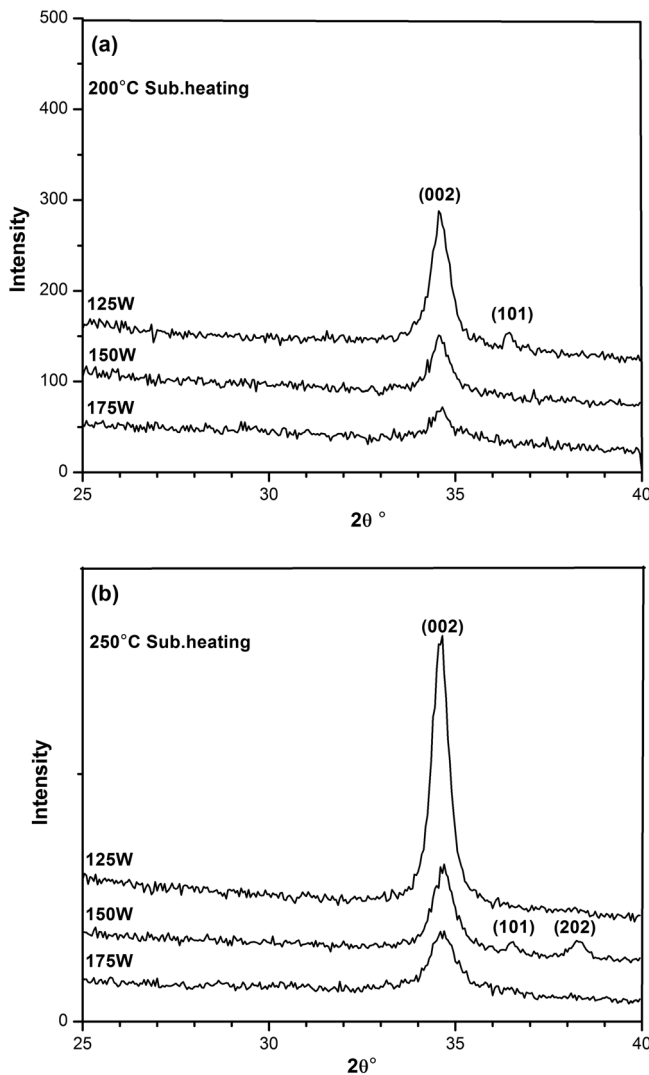


FIG. 2. Diffraction pattern for various deposition powers at (a) 200 °C and (b) 250 °C.

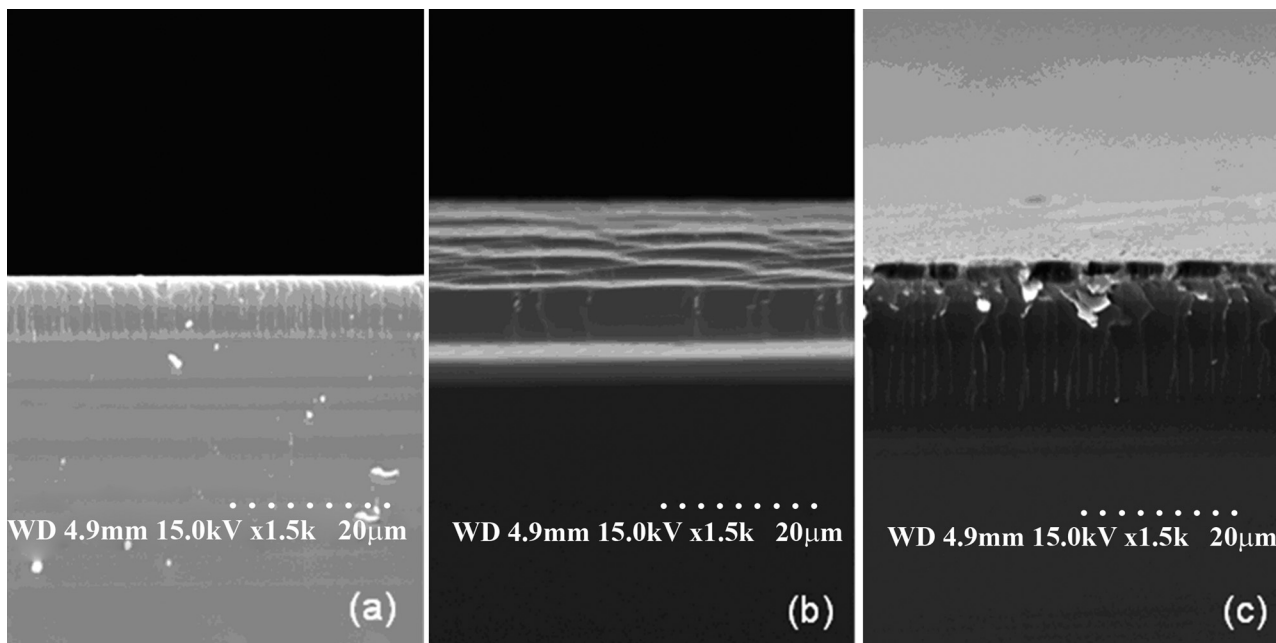


Fig. 3. SEM images of the deposited AZO films (a) 125 W at 200 °C, (b) 175 W at 200 °C, and (c) 125 W at 250 °C.

532.1 ± 0.15 eV (OIII) is attributed to loosely bonded oxygen in the surface of the AZO thin films.^{41,42} These chemisorbed oxygen impurities could be due to O²⁻, O⁻ ions.⁴⁶ The lower binding energy peak at 529.5 ± 0.15 eV (OIV) is probably due to oxygen in ZnO structure.⁴³

The relative strength of the individual O1s subpeaks, obtained by dividing the area of the particular peak by total peak area can be used to study the compositions quantitatively. Figure 6 shows the relative strength of O1s peaks for the AZO films prepared at various deposition powers and substrate temperatures. The relative strength of the O1s peaks remains almost constant for most of the films deposited at different powers. From the Fig. 6, it is evident that most of the oxygen atoms are prone to form O²⁻ ions on the

wurtzite structure of hexagonal Zn⁺ ion array for all the AZO thin films. An exception was observed at 175 W with 250 °C substrate temperature shown in Fig. 6(b) where an increase in OIV peak intensity indicated that oxygen atoms in the films were favored to form ZnAl₂O₄ and ZnO structures at higher powers.

Annealing in vacuum is considered an important process step to improve the quality of AZO films. Since oxygen content defines the electrical and optical nature of the material, we compare the high resolution oxygen peaks of the annealed samples. Figure 7 shows the high resolution deconvolution of O1s photoelectron peaks in the XPS spectra of AZO films prepared at 175 W and 250 °C substrate temperature under different annealing temperatures. It can

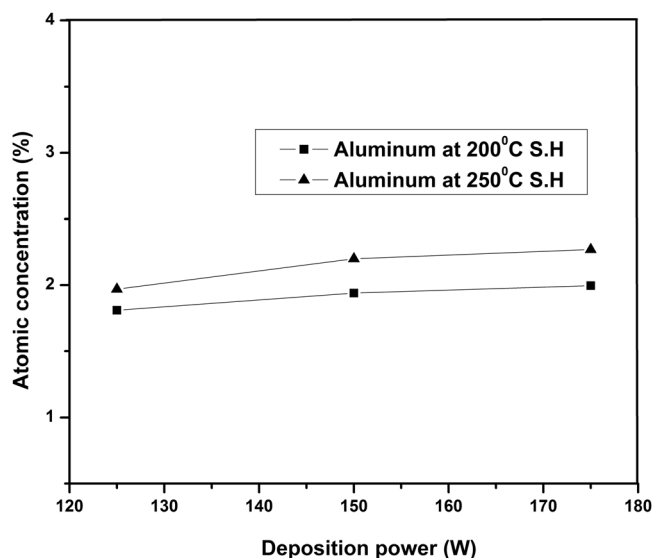


Fig. 4. Atomic concentration of aluminum with respect to various deposition power and at 200 and 250 °C deposition temperatures.

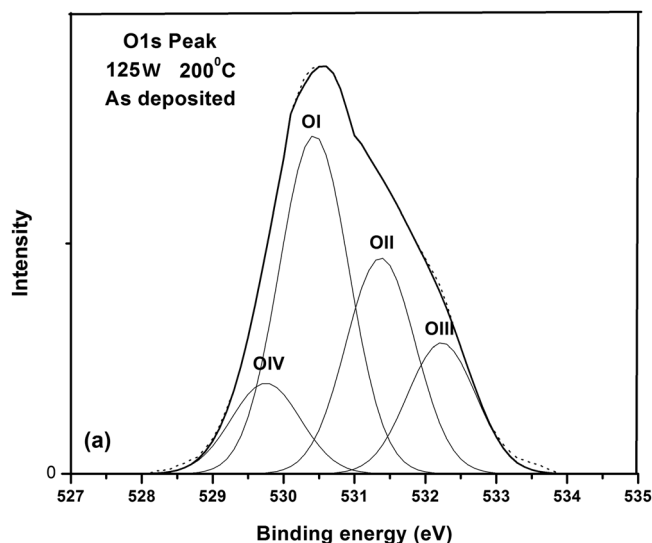


Fig. 5. O1s photoelectron peaks in the XPS spectra of AZO films prepared at 125 W and 200 °C substrate heating temperature.

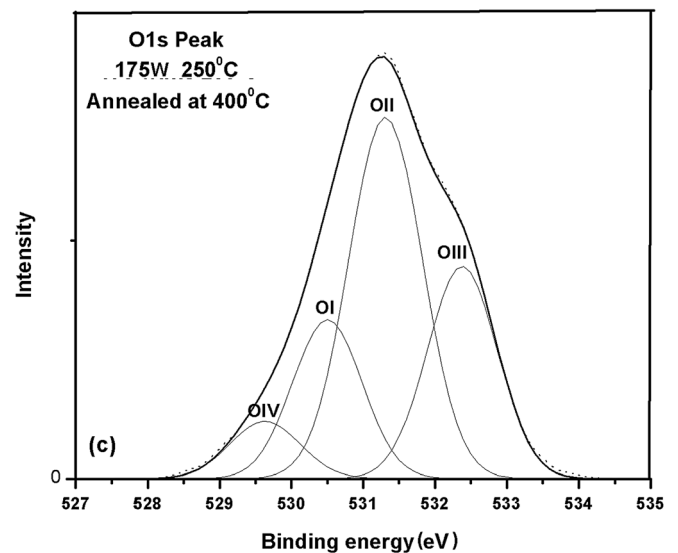
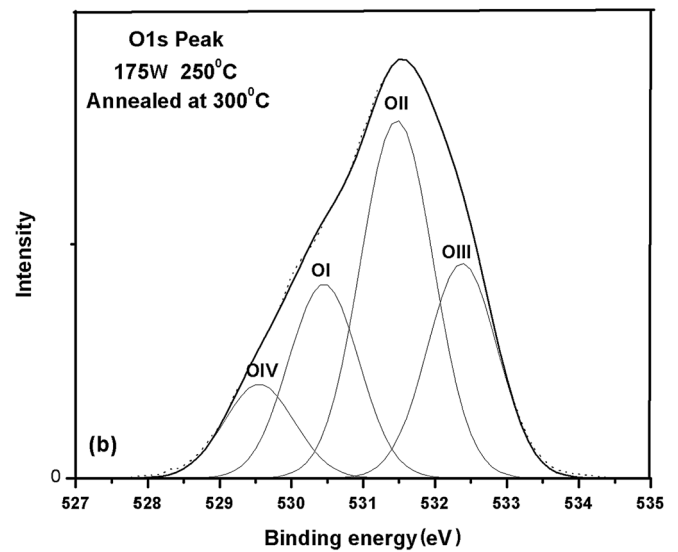
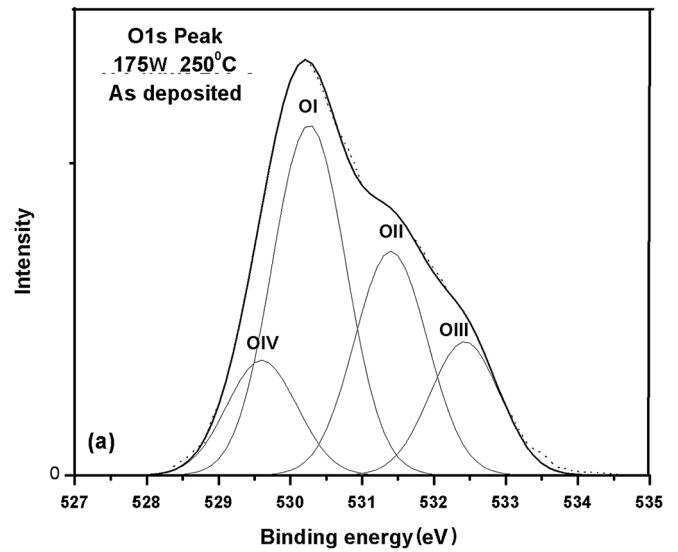
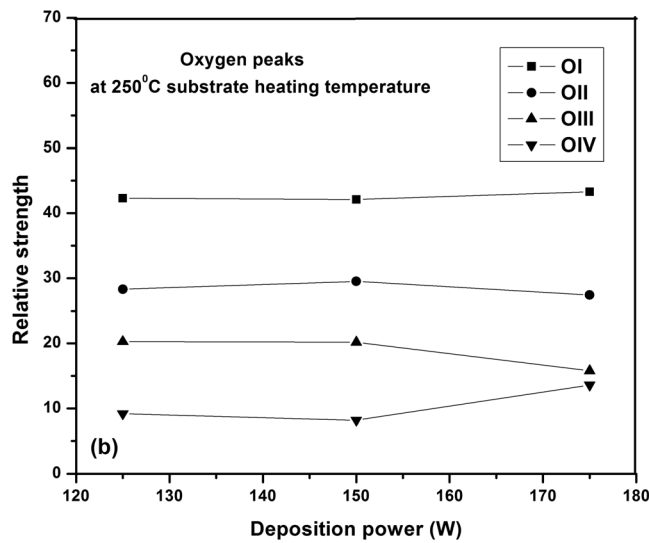
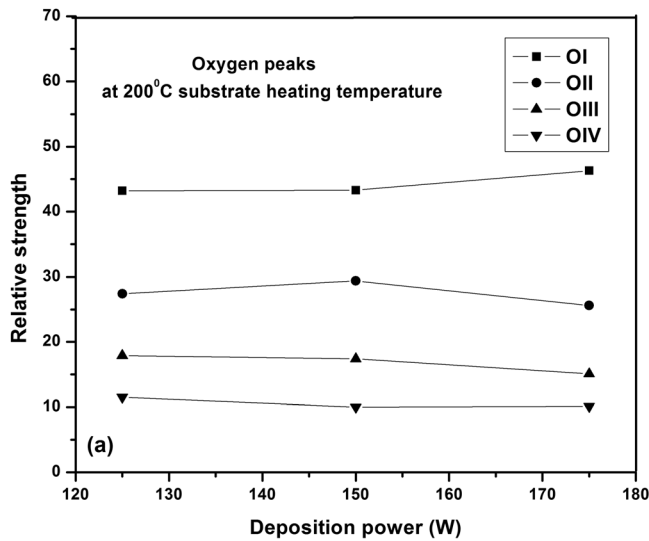


FIG. 6. Relative strengths of O1s peaks (OI, OII, OIII, and OIV) for the AZO thin film deposited at (a) 200 °C, (b) 250 °C substrate heating temperatures and varying deposition powers.

be observed that the OI peak representing the oxygen rich phase of ZnO drops at higher annealing temperatures, whereas, the peak OII representing oxygen deficiency predominant raises at higher annealing temperatures. This is the predominant peak after 400 °C anneal. This indicates a clear increase in oxygen deficiency with the increase in annealing temperatures. A more quantitative analysis can be obtained by considering the relative strength of each peak under different annealing temperatures. Figure 8 shows the relative strengths of OI, OII, OIII, and OIV peaks after vacuum annealing for the AZO films deposited at 175 W and for (a) 200 °C and (b) 250 °C substrate temperatures. It can be seen that there is a clear change in the chemical states of oxygen with the increase in annealing temperature. It is evident from the continuous decrease in relative the intensity of OI peak and continuous increases OII and OIII peaks with the increase in annealing temperature. The decrease in relative intensity of OI peak is not the only reason for increase in the relative intensity of OII and OIII peaks. It is evident that there is a

FIG. 7. O1s photoelectron peaks in the XPS spectra of AZO films prepared at (a) 175 W and 250 °C substrate heating temperature, (b) annealed in vacuum at 300 °C, (c) annealed in vacuum at 400 °C.

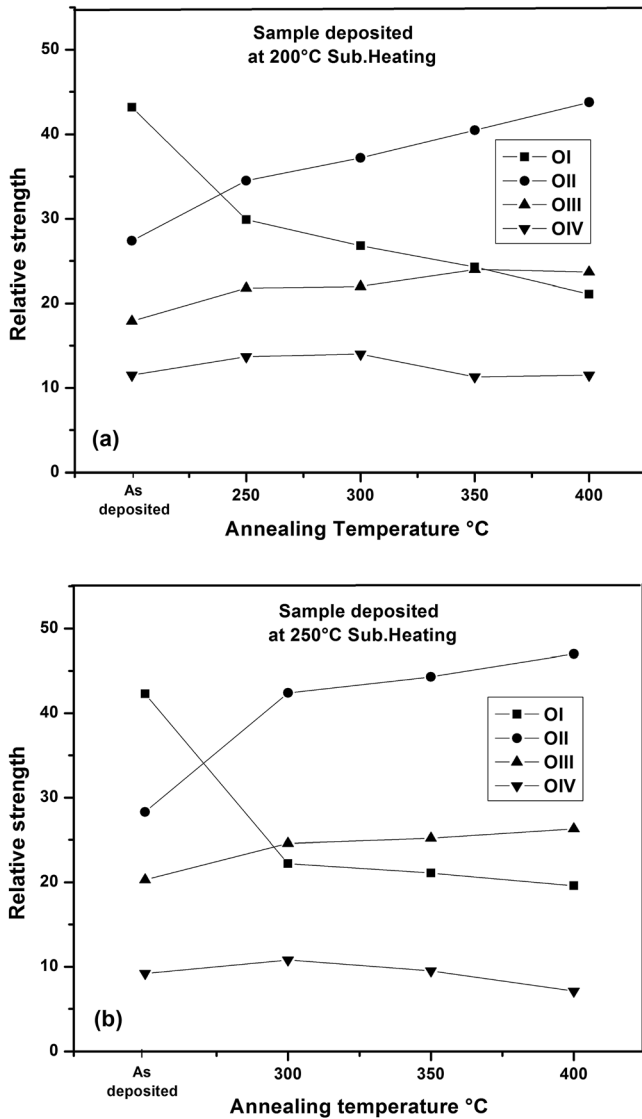


FIG. 8. Relative strengths of O1s peaks (OI, OII, OIII, and OIV) after annealing for the AZO thin film deposited at 175 W and (a) 200 °C, (b) 250 °C substrate heating temperatures.

clear change in chemical states of oxygen as there is a faster increase in the relative intensity of OII peak compared to that of OIII peak with the increase in annealing temperature. Furthermore, an increase in carrier concentration could provide direct benefit in terms of the enhancement of electrical resistivity of the films. Hence, oxygen deficient AZO thin films were obtained by annealing the sputtered films in vacuum at higher temperatures.

Low resistivity and high transparency are considered the most important figures of merit for TCO films for various applications. Figure 9(a) shows the plot of resistivity as a function of deposition powers at two substrate temperatures. Resistivity decreases continuously as the deposition power increases for the films deposited at 200 and 250 °C substrate temperatures. The AZO films deposited at higher substrate temperature of 250 °C showed lower resistivity values. The lowest resistivity value obtained was $1.15 \times 10^{-3} \Omega \text{ cm}$ for the film deposited at 175 W power and 250 °C substrate tem-

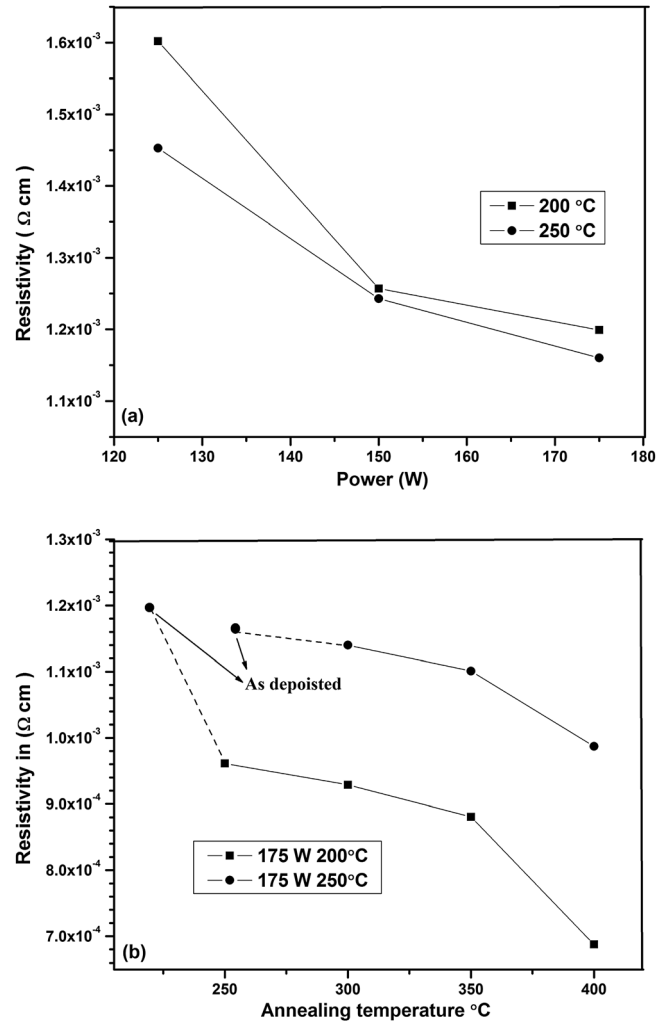


FIG. 9. Plot of resistivity for ZnO:Al thin film obtained at (a) various deposition powers and substrate heating temperatures, (b) after vacuum annealing of film obtained at 175 W for both 200 and 250 °C substrate heating temperatures.

perature. Higher power conditions are known to produce increased yield of Al in the films, which in turn provides increased carrier concentration. The higher incorporation of zinc and aluminum in the film and decrease in the amount of oxygen with deposition power and substrate heating temperatures could be the primary cause for this decrease in resistivity. This effect can be amplified by annealing under vacuum conditions as established earlier by the increased creation of oxygen deficiency in the film. Figure 9(b) shows the plot of resistivity as a function of annealing temperatures for films deposited at 175 W with substrate heated at 200 and 250 °C. It can be observed that both the films showed a decreasing trend in resistivity with increasing annealing temperatures. This is in direct correlation with the deconvolution results from chemical analysis of the films. The resistivity of the films deposited at 200 °C substrate temperature dropped more drastically with the increase in annealing temperature compared to the one deposited at 250 °C substrate temperature. The lowest resistivity of $6.67 \times 10^{-4} \Omega \text{ cm}$ was obtained for the film annealed at 400 °C. This drop in resistivity is

attributed to formation of highly oxygen deficient thin films at higher annealing temperatures. Furthermore, annealing can be expected to increase the grain sizes and film densification which could lead to reduction in grain boundary scattering thus contributing to the decrease in resistivity.

The increased Al doping and decrease in oxygen concentration could adversely affect the optical properties of the AZO film hence we consider the optical transmission measurements to optimize the deposition process conditions. Figure 10 shows the percentage optical transmission of the AZO films deposited at different RF power levels with the substrate heated at (a) 200 °C and (b) 250 °C, respectively. The films show good optical transparency in the visible region and ranging between 85–95%. It can also be observed that the transparency of the films decreases in the infrared region. Particularly, the films become more opaque in the infrared region with increasing deposition power. Since the films showing low resistivity are of particular interest we consider the optical properties of films obtained at the deposition power of 175 W. Figure 11 shows the percentage

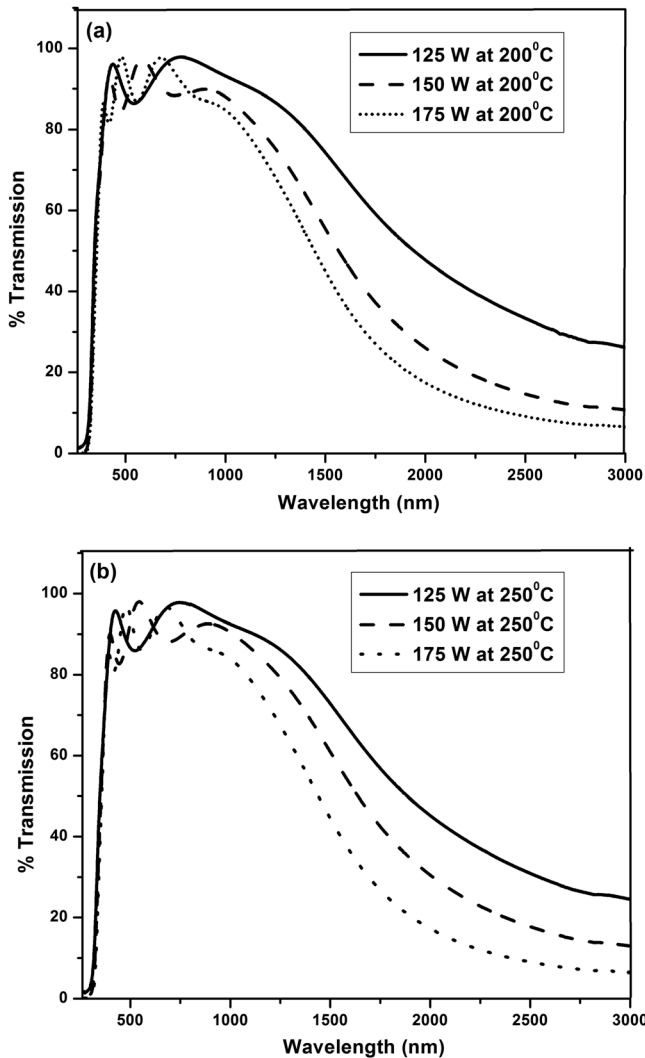


Fig. 10. Percentage transmission of the AZO thin films deposited with various deposition powers at (a) 200 and (b) 250 °C substrate heating temperatures.

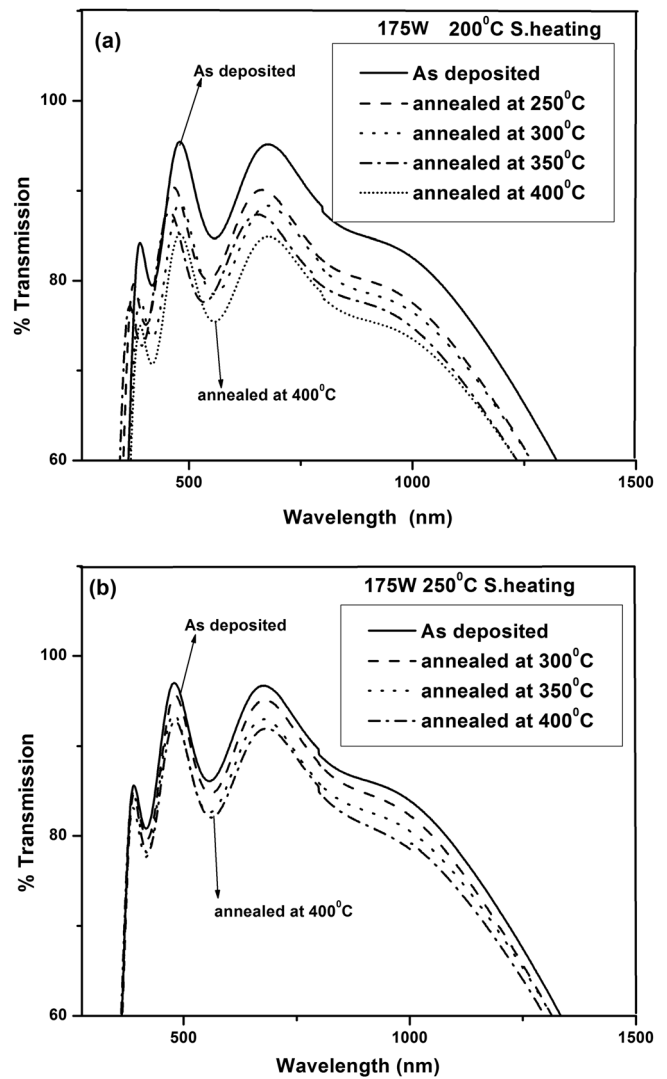


Fig. 11. Percentage transmission of the AZO thin films deposited at 175 W under (a) 200 °C and (b) 250 °C substrate heating temperatures after vacuum annealing at higher temperatures.

transmission of the annealed films deposited at 175 W and substrate temperatures of 200 and 250 °C. It can be observed that the percentage transmission of the films decreases with the increase in annealing temperatures irrespective of the substrate temperatures. This decrease in transparency with the increase in annealing temperatures can be attributed to the increase in oxygen deficiency in the films after annealing. As observed earlier, the samples annealed at higher temperatures show decreased resistivity which could directly imply increased carrier concentrations; consequently leading to lower transmission levels.

The measurement of the transmittance enables us to determine the optical refractive index of the films. The refractive index was calculated using the relations in Eqs. (1) and (2):⁴⁴

$$n(\lambda) = \frac{1}{2} \left\{ \left[8n_s c(\lambda) + (n_s + 1)^2 \right]^{1/2} + \left[8n_s c(\lambda) + (n_s - 1)^2 \right]^{1/2} \right\}, \quad (1)$$

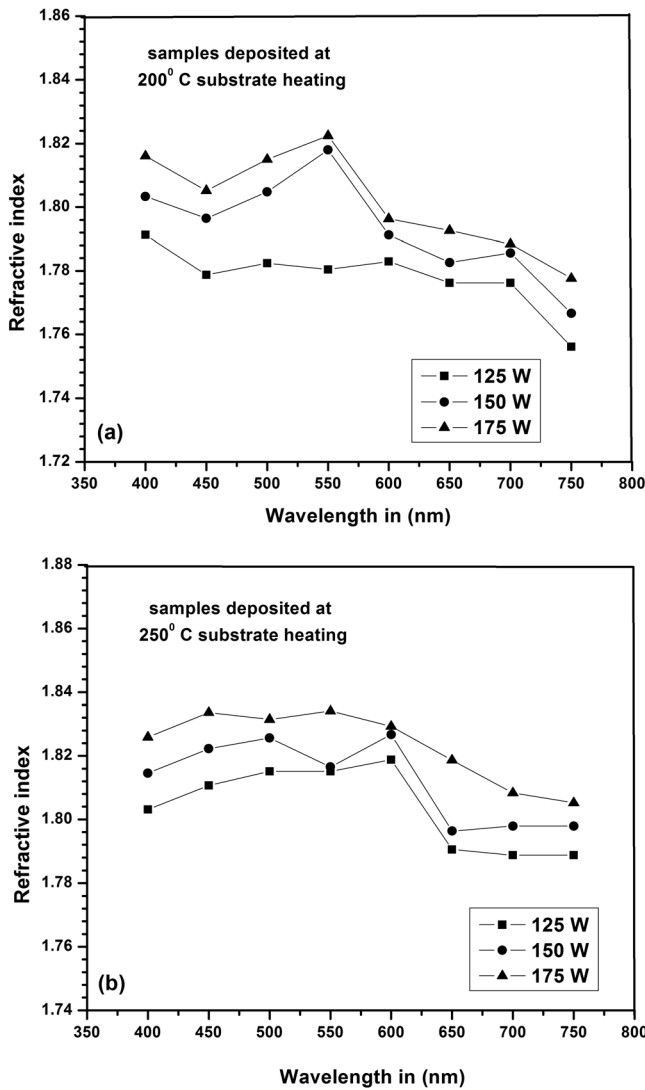


FIG. 12. Variation of refractive index n as a function of wavelength for AZO thin films deposited on glass substrate with different deposition powers with (a) 200 °C and (b) 250 °C substrate heating.

where

$$c(\lambda) = \frac{T^+(\lambda) - T^-(\lambda)}{2T^+(\lambda)T^-(\lambda)}, \tag{2}$$

where, T^+ and T^- are experimentally traced envelope curves of the transmission spectrum, and λ is the wavelength of the light and n_s is the index of refraction of the substrate. Figure 12 shows the variation of refractive index “ n ” as a function of wavelength for films deposited on glass substrates with varying power at (a) 200 °C and (b) 250 °C substrate temperatures. It can be seen that the refractive index increases with the increase in deposition power for both substrate temperatures. Figure 13 shows the variation of refractive index n as a function of wavelength for vacuum annealed films. The refractive index increases with the increase in annealing temperatures for both substrate temperatures. An opposing trend was observed by Qiao *et al.*,⁴⁵ where they report that the refractive index of the AZO films decreased as a function of

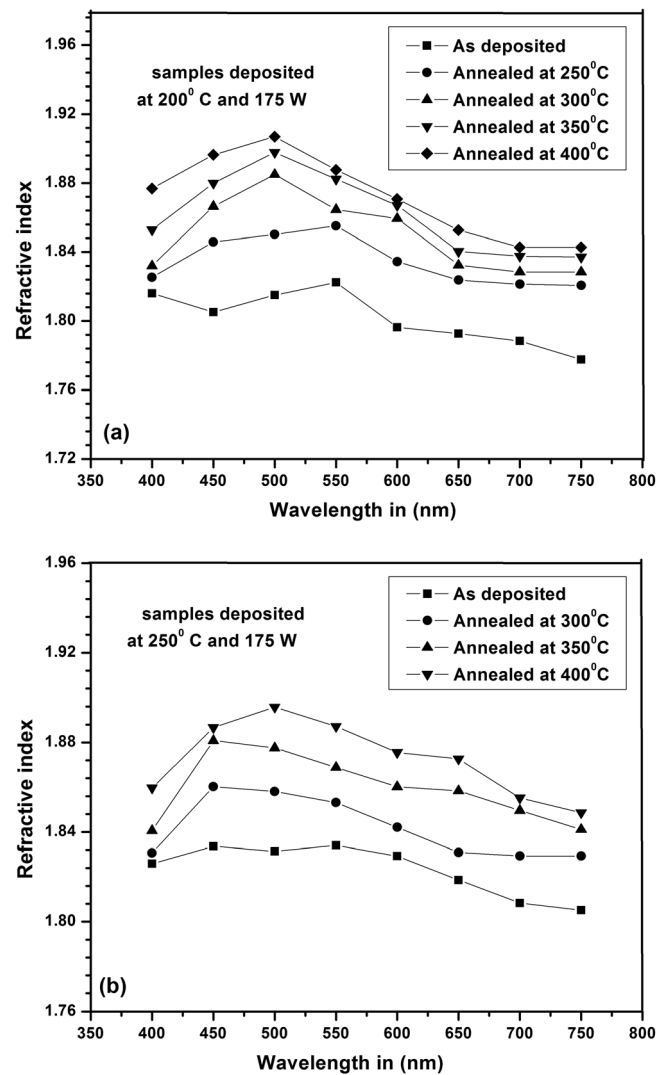


FIG. 13. Refractive index n as a function of wavelength for AZO thin films vacuum annealed at various high temperatures for a film deposited on glass corning substrate with 175 W power at (a) 200 °C and (b) 250 °C substrate heating temperature.

increasing carrier concentration. The cause for this effect is still not clearly understood yet. Further studies have to be carried out to understand this phenomenon. However, in another work reported by Ondo-Ndong *et al.*,⁴⁶ a similar increase in refractive index was observed. In their study, film deposited at 250 °C had a higher refractive index than the film deposited at 200 °C.

IV. CONCLUSION

Aluminum doped zinc oxide thin films were prepared by RF sputtering from an alumina doped zinc oxide target, using different deposition powers and substrate temperatures. Chemical analysis of the oxygen states has revealed significant correlation between the oxygen deficiency in the films and the electrical and optical properties. Increase in deposition power increases the incorporation of aluminum in the film. It also causes increase in oxygen deficiency at higher substrate temperatures which is the main reason for

the decrease in resistivity of the AZO films. Annealing of the film deposited at 175 W in vacuum caused significant decrease in resistivity of the AZO thin films. XPS results show that this decrease in resistivity is due to increase in oxygen deficiency in the film after annealing. The films obtained were found to be polycrystalline with the prominent orientation (002) perpendicular to the substrate surface where crystallinity increases with the increase in substrate temperature and decreased with the increase in deposition power. The AZO films obtained at higher powers have good transparency in visible region. The film with lowest resistivity of $6.67 \times 10^{-4} \Omega \text{ cm}$ and transparency greater than 90% was obtained at deposition power of 175 W and substrate temperature of 200 °C after vacuum annealing at 400 °C.

- ¹K. L. Chopra, S. Majors, and D. K. Pandya, *Thin Solid Films* **102**, 1 (1983).
- ²A. L. Dawar and J. C. Joshi, *J. Mater. Sci.* **19**, 1 (1984).
- ³R. G. Gordon, *MRS Bull.* **25**, 52 (2000).
- ⁴J. F. Carlin, Jr., U.S. Geological Survey, Mineral Commodity Summaries, January, 2006.
- ⁵T. Minami, H. Nanto, and S. Takata, *Jpn. J. Appl. Phys.* **23**, L280 (1984).
- ⁶A. Malik, A. Seco, R. Vieira, E. Fortunato, and R. Martins, *MRS Proc.* **471**, 47 (1997).
- ⁷E. Shanti, A. Banerjee, and K. L. Chopra, *Thin Solid Films* **108**, 333 (1983).
- ⁸H. Sato, T. Minami, S. Takata, T. Miyata, and M. Ishii, *Thin Solid Films* **236**, 14 (1993).
- ⁹J. Hu and R. G. Gordon, *J. Appl. Phys.* **71**, 880 (1992).
- ¹⁰B. P. Zhang, K. Wakatsuki, N. T. Binh, N. Usamic, and Y. Segawa, *Thin Solid Films* **449**, 12 (2004).
- ¹¹A. Suzuki, T. Matsushita, N. Wada, Y. Sakamoto, and M. Okuda, *Jpn. J. Appl. Phys.* **35**, L56 (1996).
- ¹²H. Kim, C. M. Gilmore, J. S. Horwitz, A. Piqué, H. Murata, G. P. Kushto, R. Schlaf, Z. H. Kafafi, and D. B. Chrisey, *Appl. Phys. Lett.* **76**, 259 (2000).
- ¹³T. Minami, H. Sato, H. Imamoto, and S. Takata, *Jpn. J. Appl. Phys.* **31**, L257 (1992).
- ¹⁴D. Goyal, P. Solanki, B. Marathe, M. Takwale, and V. Bhide, *Jpn. J. Appl. Phys.* **31**, 361 (1992).
- ¹⁵D. H. Zhang and E. D. Brodie, *Thin Solid Films* **238**, 95 (1994).
- ¹⁶A. Kuroyanagi, *Jpn. J. Appl. Phys.*, Part 2 **28**, L219 (1989).
- ¹⁷M. J. Alam and D. C. Cameron, *J. Vac. Sci. Technol. A* **19**, 1642 (2001).
- ¹⁸T. Tsuchiya, T. Emoto, and T. Tadanori, *J. Non-Cryst. Solids* **178**, 327 (1994).
- ¹⁹H. L. Hartnagel, A. L. Dawar, A. K. Jain, and C. Jagadish, *Semiconducting Transparent Thin Films* (Institute of Physics, Philadelphia, 1995).
- ²⁰T. Minami, H. Nanto, and S. Takata, *Appl. Phys. Lett.* **41**, 958 (1982).
- ²¹T. Minami, K. Oohashi, S. Takata, T. Mouri, and N. Ogawa, *Thin Solid Films* **193–194**, 721 (1990).
- ²²O. Kluth, G. Schope, B. Rech, R. Menner, M. Oertel, K. Orgassa, and H. W. Schock, *Thin Solid Films* **502**, 311 (2006).
- ²³K. H. Kim, K. C. Park, and D. Y. Ma, *J. Appl. Phys.* **81**, 7764 (1997).
- ²⁴C. Agashe, O. Kluth, J. Hüpkes, U. Zastrow, and B. Rech, *J. Appl. Phys.* **95**, 1911 (2004).
- ²⁵G. Fang, D. Li, and B. L. Yao, *Vacuum* **68**, 363 (2002).
- ²⁶M. Berginski, J. Hupkes, W. Reetz, B. Rech, and M. Wuttig, *Thin Solid Films* **516**, 5836 (2008).
- ²⁷M. Chen, X. Wang, Y. H. Yu, Z. L. Pei, X. D. Bai, C. Sun, R. F. Huang, and L. S. Wen, *Appl. Surf. Sci.* **158**, 134 (2000).
- ²⁸G. J. Fang, D. Li, and B.-L. Yao, *Thin Solid Films* **418**, 156 (2002).
- ²⁹J. G. Lu and S. Fujita, *J. Appl. Phys.* **101**, 083705 (2007).
- ³⁰J. G. Lu, Z. Z. Ye, Y. J. Zeng, L. P. Zhu, L. Wang, J. Yuan, and B. H. Zhao, *J. Appl. Phys.* **100**, 073714 (2006).
- ³¹F. C. M. Van De Pol, F. R. Blom, and Th. J. A. Popma, *Thin Solid Films* **204**, 349 (1991).
- ³²M. Jin, J. Feng, Z. De-heng, M. Hong-lei, and L. Shu-ying, *Thin Solid Films* **357**, 98 (1999).
- ³³K. B. Sundaram and A. Khan, *Thin Solid Films* **295**, 87 (1997).
- ³⁴M. Dinescu and P. Verardi, *Appl. Surf. Sci.* **106**, 149 (1996).
- ³⁵J. A. Thornton, *J. Vac. Sci. Technol.* **11**, 666 (1974).
- ³⁶O. Kluth, G. Schope, J. Hupkes, C. Agashe, J. Muller, and B. Rech, *Thin Solid Films* **442**, 80 (2003).
- ³⁷R. Cebulla, R. Weridt, and K. Ellmer, *J. Appl. Phys.* **83**, 1087 (1998).
- ³⁸T. Szorenyi, L. D. Laude, I. Bertoti, Z. Ka'ntor, and Z. Ge're-tovszky, *J. Appl. Phys.* **78**, 6211 (1995).
- ³⁹T. L. Yang, D. H. Zhang, J. Ma, H. L. Ma, and Y. Chen, *Thin Solid Films* **326**, 60 (1998).
- ⁴⁰Y. J. Kim and H. J. Kim, *Mater. Lett.* **41**, 159 (1999).
- ⁴¹M. N. Islam, T. B. Ghosh, K. L. Chopra, and H. N. Acharya, *Thin Solid Films* **280**, 20 (1996).
- ⁴²S. Major, S. Kumar, M. Bhatnagar, and K. L. Chopra, *Appl. Phys. Lett.* **40**, 394 (1986).
- ⁴³V. E. Henrich and P. A. Cox, *The Surface Science of Metal Oxides* (Cambridge University Press, New York, 1994).
- ⁴⁴H. Demiryont, J. R. Sites, and K. Geib, *Appl. Opt.* **24**, 490 (1985).
- ⁴⁵Z. Qiao, C. Agashe, and D. Mergel, *Thin Solid Films* **496**, 520 (2006).
- ⁴⁶R. Ondo-Ndong, F. Pascal-Delannoy, A. Boyer, A. Giani, and A. Foucaran, *Mater. Sci. Eng. B* **97**, 68 (2003).